The incorporation of nitrosocyanin copper binding loop into azurin

A THESIS
SUBMITTED TO THE FACULTY OF THE GRADUATE SCHOOL
OF THE UNIVERSITY OF MINNESOTA
BY

Audrey Rose Schenewerk

IN PARTIAL FULFILLMENT OF THE REQUIREMENTS
FOR THE DEGREE OF
MASTER OF SCIENCE

Dr. Steven M. Berry

July 2010

Acknowledgements

I would like to thank Dr. Steven Berry for this opportunity and his guidance over the past two years. I would also like to thank my friends and family for their support. I have received help from other students, and I would specifically like to thank Erika Bladholm, Madelyn Baker, Melanie Halverson, Chuhan Zong, Andy McCabe and Greg Reynolds. Finally, I would like to thank the Department of Chemistry and Biochemistry for making this opportunity possible.

ABSTRACT

Metalloprotein design and engineering can be used to probe our understanding of active site structure and function. Loop-directed mutagenesis has been used in the metalloprotein field to change the copper binding loops from a number of members of the cupredoxin family into other protein scaffolds. We report the replacement of a ten amino acid loop that supports the copper binding site in the blue copper protein azurin with the red copper binding loop from the protein nitrosocyanin. Azurin is an electron transfer protein while the role of nitrosocyanin is unknown, yet believed to be catalytic. In addition to the loop, we added a carboxylic acid residue into the copper binding site which fully models the site of nitrosocyanin. Synthesis, expression, and UV-visible absorption and EPR spectra for this series of azurin variants will be reported.

TABLE OF CONTENTS

ACKNOWLEDGEMENTS i
ABSTRACT ii
LIST OF TABLES iv
LIST OF FIGURES v

CHAPTER 1: INTRODUCTION 2
1.1 METALLOPROTEINS 2
1.2 AZURIN 4
1.3 NITROSOCYANIN 7
1.4 NC AND AZ COMPARISON 10
1.5 LOOP DIRECTED MUTAGENESIS 13

CHAPTER 2: DESIGN AND SYNTHESIS OF NITROSOCYANIN AZURIN MUTANT 17
2.1 MUTAGENESIS OF AZURIN TO INCORPORATE NITROSOCYANIN LOOP 13
2.2 DESIGN OF HIS46 TO GLU MUTATION 18
2.3 HIS46 TO ASP MUTAGENESIS 20
2.4 PROTEIN EXPRESSION AND PURIFICATION 21
2.5 PREPARING EPR SAMPLES AND DETERMINING ABSORPTIVITY 23

CHAPTER 3: PROTEIN CHARACTERIZATION 24
3.1 INTRODUCTION 24
3.2 MUTAGENESIS RESULTS 24
3.2.1 LOOP MUTAGENESIS 24
3.2.2 HIS46 TO GLU MUTAGENESIS 26
3.2.3 HIS46 TO ASP MUTAGENESIS 26
3.3 PROTEIN PURIFICATION RESULTS 27
3.4 UV-VISIBLE SPECTROSCOPY 29
3.4.1 LOOP ABSORPTION SPECTROSCOPY 29
3.4.2 WTH46E ABSORPTION SPECTROSCOPY 30
3.4.3.WTH46D ABSORPTION SPECTROSCOPY 30
3.4.4.NCH46D ABSORPTION SPECTROSCOPY 31
3.5 EPR SPECTROMETRY AND DETERMINING MOLAR ABSORPTIVITY 32

CHAPTER 4: ACTIVITY ASSAYS 35
4.1 ACTIVITY ASSAYS FOR NITROSOCYANIN 35
4.2 SOD ACTIVITY ASSAY 36
4.3 SOD ASSAY EXPERIMENTAL DETAILS 38
4.4 SOD RESULTS 39

CHAPTER 5: NATIVE NITROSOCYANIN AND DESIGNED MUTANT COMPARISON 46

REFERENCES 48

LIST OF TABLES

TABLE 1:Protein yields of WT Az, WTH46D, Loop and NCH46D. Each yield was from a 4 L growth……28

TABLE 2: Reports $g_{//}$ and $A_{//}$ values of WT Az, native nitrosocyanin, WTH46D, Loop and NCH46D……33

TABLE 3: SOD Assay reagents and the specific order and concentration. ……..39

TABLE 4: SOD Assay Δ550 nm and rate of superoxide degradation……..45

LIST OF FIGURES

FIGURE 1: Azurin crystal structure (PDB ID: 4AZU) 5
FIGURE 2: Azurin active site 6
FIGURE 3: Nitrosocyanin monomer crystal structure (PDB ID: 1IBY) 8
FIGURE 4: Nitrosocyanin active site 8
FIGURE 5: The nitrogen cycle 10
FIGURE 6: Loop directed mutagenesis 11
FIGURE 7: Azurin and nitrosocyanin structural comparison 12
FIGURE 8: SmaI cut sites in WT Az compared to Az with NC loop incorporated 18
FIGURE 9: Forward and reverse primer for His46 to Glu mutation 19
FIGURE 10: Forward and reverse primers for His46 to Asp mutation 20
FIGURE 11: His46 to Asp mutation and Btg1 elimination 21
FIGURE 12: 1% agarose gel of SmaI restriction digest 25
FIGURE 13: 1% agarose gel of Btg1 restriction digest 27
FIGURE 14: 12% SDS PAGE results of Loop purification 29
FIGURE 15: WT Az and WTH46D UV-visible absorption spectra overlay 30
FIGURE 16: WT Az and Loop mutant UV-visible absorption spectra overlay 31
FIGURE 17: NCH46D compared to Loop UV/visible spectra 32
FIGURE 18: EPR spectra of WT Az, Loop, WTH46D and NCH46D 33
FIGURE 19: Loop, 1 mM Cu(II), 1 mM WT Az and 0.5 mM WT Az spectra to determine loop molar absorptivity 34
FIGURE 20: Fully reduced cytochrome c 37
FIGURE 21: Superoxide dismutase reaction scheme 37
FIGURE 22: Negative control, positive control, $CuSO_4$ and azurin SOD assays 41
FIGURE 23: WT Az SOD assay 41
FIGURE 24: H46D mutant SOD assays 43
FIGURE 25: Comparison at 550 nm of negative and positive controls, Cu(II), Cu/Zn SOD, WTH46D and NCH46D 44

CHAPTER 1: INTRODUCTION

1.1 METALLOPROTEINS

Metals are natural cofactors of many proteins, such as amylases, that are required to perform biological and industrial processes.[1-2] The protein activity depends on the coordination of a specific metal ion. These metalloproteins have active centers that are able to catalyze reactions from electron transfer in copper binding azurin to the dismutations of copper-zinc enzyme superoxide dismutase or the peroxide reducing heme-protein, catalase.[3]

Studying these metalloproteins with a model protein is one method of better understanding their structure function relationships. Using a model protein and incorporating various mutations in order to recreate the active site of another protein allows for increased understanding of the designed active site.[4-6] Understanding metalloprotein design could be used to improve the efficiency of industrial catalysts but more simply to understand the structure function relationship of a native metalloprotein.

The metalloproteins of interest in this thesis bind copper in the active site. There are four primary types of copper binding proteins each with different geometry, enabling copper to be an important and diverse metal in biology. Each class of copper binding protein is identified by function, spectroscopic data, and ligand coordination geometries. The first class of copper proteins, type 1 or blue copper proteins, have a copper ion with a trigonal planar geometry coordinated by two His and a Cys and often with one or two axial ligands typically a carbonyl

or thioether group. They are typically involved in electron transfer and are called cupredoxins because they are a family of copper proteins capable of catalyzing redox reactions.[6-7] Their characteristic β-barrel greek key motif is thus known as the cupredoxin fold.[8] Blue copper proteins gain their name from the observed blue color resulting from an intense charge transfer band at about 600 nm when copper is in the oxidized or Cu(II) state. The blue copper proteins have a characteristic narrow hyperfine coupling in the parallel region of their electron paramagnetic resonance (EPR) spectrum. Plastocyanin, azurin, pseudoazurin and amicyanin are examples of type 1 copper binding proteins.[9] A second class of copper proteins is Type 2 copper proteins. These are also mononuclear copper proteins with four or five copper binding ligands typically, His, Cys and Asp or Glu residues and substrate, creating a square planar or square pyramidal geometry, respectively. Such proteins like nitrite reductase, galactose oxidase and peptidyl α-hydroxylating monooxygenase typically have a catalytic function and can be identified by their broad hyperfine coupling in EPR spectrum, compared to that of type 1 copper binding protein.[3,8,10] Type 2 copper proteins are weakly blue colored and generally do not have a single identifying UV-vis charge transfer band.[7] A third class of copper proteins is the type 3 dinuclear copper protein such as tyrosinase. The copper ions in these proteins are coordinated by three ligands and an additional bridging ligand, typically a hydroxyl or O_2.[7,11] The coupled coppers do not give an EPR signal because they are antiferromagnetically coupled.[7,12] They do show a strong charge transfer band in UV-visible absorption spectra near 330 nm.[7] The final class of copper

center, Cu_A, is also an electron transfer type of copper binding protein, found in proteins such as cytochrome c oxidase.[13] These proteins are dinuclear with two Cys bridging the copper ions and each with an individual His as well as an axial ligand. Cu_A proteins often have a nice purple color due to the ligand to metal charge transfer. These proteins also have unusual EPR parallel regions where seven hyperfines are present resulting from the coupled copper in the active site.[14-15] Copper binding proteins can generally be categorized into one of these four groups based on spectroscopy, geometry and function; however there are some copper centers that have characteristics of more than one copper class.

1.2 AZURIN

The type one copper binding protein azurin, found in *Pseudomonas aeruginosa* is a well characterized stable protein. Azurin functions as an electron transfer protein with a number of redox partners such as cytochrome c_{551}, dehydrogenases, nitrite reductase, cytochrome c peroxidase and potentially other proteins involved in energy metabolism.[8,16] The reduction potential of azurin is ~+320 mV vs SHE.[9,17] This protein has a greek key β-barrel motif also known as the cupredoxin motif common to many blue copper proteins.[6] Azurin is a 14 kDa protein with 128 residues.[18-19] (Fig 1) There is an additional 19 residue peptide on the N terminus found in the azurin proprotein which is likely a leader sequence to move the protein into the periplasm. Once in the periplasm the protein is processed resulting in an apo-azurin protein.[20] The active site is typical of blue copper proteins where the copper is coordinated by His46, His117 and

Cys112 in the equatorial plane and weak axial ligands Met121 and the backbone carbonyl of a Gly45 residue maintaining a trigonal bipyramidal geometry.[12] (Fig 2) The protein has been crystallized to 1.90 Å at pH 5.5 by Nar in 1991.[18] The structure revealed unique metal to ligand bond distances. The His ligands had the shortest bond lengths where the Cu-N on His 117 and His 46 were 2.03 Å and 2.11 Å respectively and the remaining equatorial ligand, Cys 112, had a S-Cu bond distance of 2.25 Å. The weak axial ligands maintained longer bond distances with the Cu ion. Gly 45 to Cu bond distance was 2.97 Å and the Met 121 length was 3.15 Å.[18,21] Ligand coordination with the Cu(II) ion in the active site gives the protein a unique intense blue color.

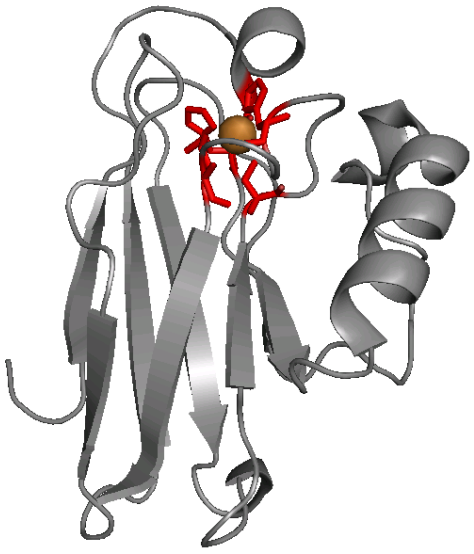

Figure 1 Azurin crystal structure (PDB ID: 4AZU). The cupredoxin fold is shown encasing the active site where the red structures identify the ligands coordinated to the copper which is the blue sphere.

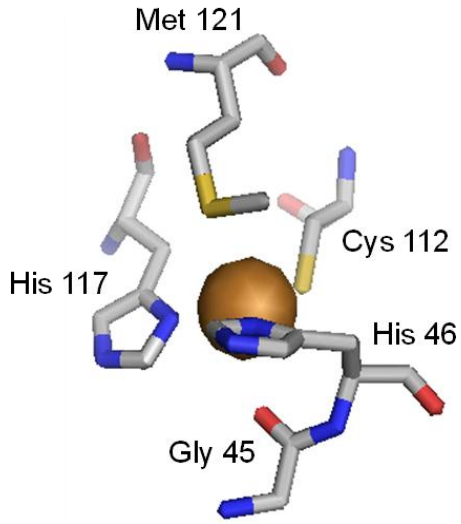

Figure 2 Azurin active site. The copper atom in azurin is coordinated by 3 strong equatorial ligands (His46, His117 and Cys112) and two weak axial ligands (Met121 and carbonyl of Gly45).

The well known intense blue color is from the strong Cys-S(π) to Cu(II) charge transfer seen in UV-visible absorption spectrum at ~625 nm with a molar absorptivity of ~5000 $M^{-1}cm^{-1}$.[21] This strong band is a result of the highly covalent, shared electron density of the Cys(S)-Cu(II) bond. Azurin has been identified by its narrow hyperfine coupling constant of 58 G in EPR spectrometry, from the shared electron density, and a $g_{//}$ value of 2.23.

The azurin gene has been subcloned from *P. aeruginosa* into an *E. coli* plasmid vector.[22] By placing the gene under the control of the *lac* promoter, induction can easily be performed with use of isopropyl-β-D-1-thiogalactopyranoside (IPTG).[23] This allows for ready expression and purification, and has made the protein an ideal scaffold candidate for metalloprotein design to model other copper binding proteins.[24]

1.3 NITROSOCYANIN

The copper binding protein nitrosocyanin is native to *Nitrosomonas europaea*, an ammonia-oxidizing autotrophic bacterium found in soil and other nitrogen rich environments. It is a trimer of mononuclear cupredoxin 12 kDa monomers in solution and identified as a trimer crystallographically. Each monomer is 112 residues in length.[25-26] Nitrosocyanin contains the same β-barrel and cupredoxin fold and is significantly homologous to blue copper proteins plastocyanin, azurin and rusticyanin.[27] (Fig 3) The copper active site found in each monomer does not identify with a single copper protein class.[25] The copper is coordinated in the active site by five ligands, His98, His103, Cys95, Glu60 and an axial water or substrate molecule, forming a square pyramidal geometry.[28] (Fig 4) The 1.65 Å resolution crystal structure (PDB ID: 1IBY) measured bond lengths for the equatorial ligands His98, His103, Cys95 and Glu60 as 2.02 Å, 1.97 Å, 2.26 Å and 2.09 Å, respectively while the axial ligand, water, has a distance of 2.25 Å.[25] This geometry contributes to the unique spectroscopy of the protein.

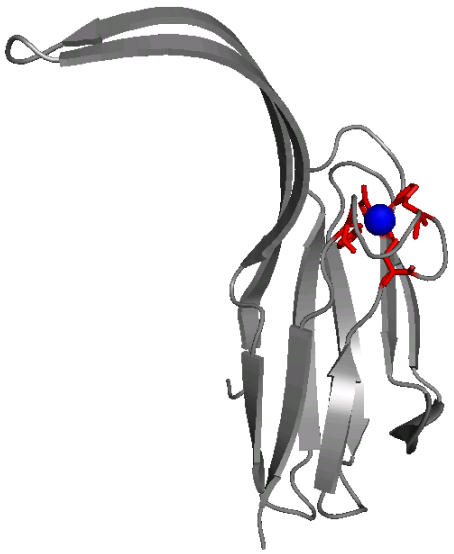

Figure 3 Nitrosocyanin monomer crystal structure (PBD ID: 1IBY). Cupredoxin fold typical of blue copper proteins is visible. The active site residues are depicted in red and the blue sphere indicates the copper ion.

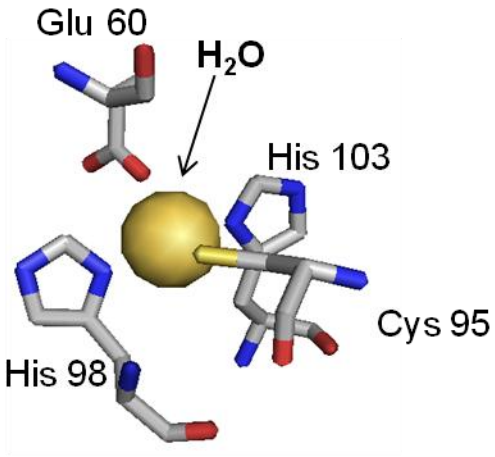

Figure 4 Nitrosocyanin active site. The copper ion in nitrosocyanin is coordinated by five ligands (His98, Cys 95, His 103, Glu60 and a water molecule). The copper ion is indicated by the gold sphere.

Nitrosocyanin has distinct spectroscopic characteristics which give rise to its red color and are noticeably different from blue copper proteins as well as perturbed blue copper proteins, such as cucumber basic or nitrite reductase which both have a green-blue color.[9,29] UV-visible absorption spectroscopy of nitrosocyanin detects bands at 390 (ε= ~7000 $M^{-1}cm^{-1}$), 496 and 720 nm which have been assigned as Cys-S(σ) to Cu(II) charge transfer, Cys-S(π) to Cu(II) charge transfer and d to d transitions, respectively.[9,27-28] The parallel region of the EPR spectrum for nitrosocyanin gives a broad copper hyperfine coupling constant ($A_{//}$ ~ 137 G) and $g_{//}$ of 2.25. This is a distinct difference from the EPR spectra of cupredoxins and is more similar to that of type 2 copper proteins. The reduction potential (+85 mV vs SHE) is much lower than typical type 1 copper proteins (+184 to +680 vs. NHE) and also more similar to the reduction potential of a catalytically active type 2 copper protein.[27,30] The geometry of the Cu center and the presence of an open binding site for water or substrate also suggest a catalytic function for the protein which is more typical of the type 2 copper proteins.[7]

The bacterium *N. europaea* is known to produce energy from aerobic oxidation of ammonia to nitrite.[29] Nitrosocyanin has been found at concentrations similar to other enzymes essential to *N. europaea*, particularly those involved in ammonia oxidation within the nitrogen cycle.[25,31] (Fig 5) Under hypoxic conditions *N. europaea* can produce significant levels of NO and N_2O as well as trace levels of N_2 gas during denitrification of NO_3^-.[32] The reduction of NO_2^- produces toxic NO in vivo, where a type 2 copper enzyme, called NirK, has

been found to have nitrite reductase activity. However, in the absence of this enzyme denitrification still occurs, suggesting an alternative pathway.[29,33] Further study of this bacterium is necessary in order to determine nitrosocyanin's possible role in ammonia oxidation or other processes in the bacterium.

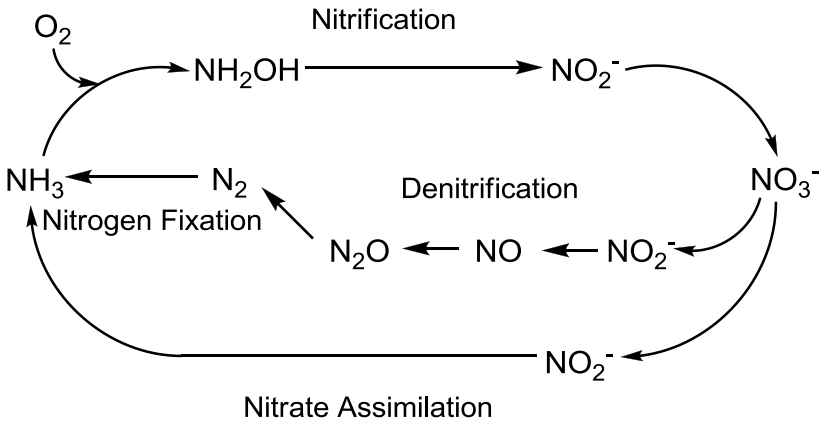

Figure 5 The Nitrogen Cycle. The cycle shows NH_3 oxidation to NO_3^- in the nitrification process followed by the reduction of NO_3^- through denitrification to N_2 or nitrate assimilation producing NH_3.

1.4 NC AND AZ COMPARISON

In a blast search, nitrosocyanin's C-terminus was found to have ~65% sequence homology to plastocyanin and similarities to the cupredoxins azurin, pseudoazurin, amicyanin and rusticyanin.[27] The sequence homology and structural similarity of nitrosocyanin and azurin makes azurin an excellent scaffold for metalloprotein design. We know the cupredoxin motif of azurin holds the active site rigidly and adds to azurin's stability. Thus, azurin can be used to accurately model the active site of nitrosocyanin. The active site loop of nitrosocyanin is different from that of azurin. The 10 residue loop of nitrosocyanin is ^{95}**Cys**GlnLeu**His**ProLysAsnIle**His**Leu^{104}, containing three of the

copper binding ligands, Cys95 His98, His103.[27] This can be compared to azurin's 10 residue copper binding loop ^{112}**Cys**ThrPheProGly**His**SerAlaLeu**Met**^{120}. (Fig 6 and 7) Both loops have a Cys residue immediately before the loop sequence which is involved in copper coordination at the active site. We want to look at the structural and functional changes that occur when the azurin active site loop is replaced with that of nitrosocyanin.

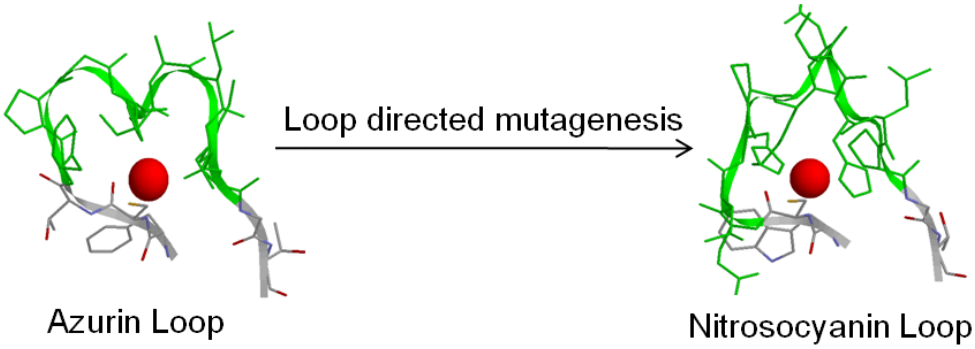


```
                        112 113                          122
Azurin Loop: …PhePheCys ThrPheProGlyHisSerAlaLeuMetLys GlyThrLeu…

                         95 96                          105
NC Loop:      …IleTrpCys GlnLeuHisProLysAsnIleHisLeuPro GlyThrLeu…
```

Figure 6 Loop directed mutagenesis. This mutagenesis incorporated the nitrosocyanin loop residue 96 through 105 into azurin replacing its native loop residues 113 through 122.

Figure 7 Azurin and Nitrosocyanin Structural Comparison. On the left azurin (PBD ID: 4AZU) and the right, nitrosocyanin (PDB ID: 1IBY) crystal structures show the similar cupredoxin motif but differing location of copper binding loop.

The spectroscopic data of blue copper protein and red copper protein were compared. A number of spectroscopic differences have been identified despite their similar structure and active site coordination.[9,28] The UV-visible absorption spectrum of oxidized azurin shows an intense Cys(S)π→Cu(II) charge transfer band at 625 nm and weaker Cys(S)σ→Cu(II) charge transfer band at 480 nm as well as d→d transitions at lower energy. The strong Cys(S)π→Cu(II) charge transfer band is the reason for the brilliant blue color of azurin. In the nitrosocyanin spectrum there is a Cys(S)σ→Cu(II) charge transfer band at 390 nm which gives rise to the red color of this protein there is also a weak Cys(S)π→Cu(II) band at ~500 nm and d→d transitions at 720 nm. The Cys(S)π→Cu(II) charge transfer bands of azurin and the Cys(S)σ→Cu(II) of nitrosocyanin have molar absorptivities of 5000 $M^{-1}cm^{-1}$ and 7000 $M^{-1}cm^{-1}$, respectively.[9,27-28,34] The Cys(S)π→Cu(II) and d→d transitions of nitrosocyanin

have molar absorptivities of 2200 $M^{-1}cm^{-1}$ and 900 $M^{-1}cm^{-1}$,[27] while the Cys(S)σ→Cu(II) charge transfer band in azurin has a molar absorptivity of 200 $M^{-1}cm^{-1}$.[8] The parallel region in EPR spectra for each protein differs greatly. The azurin spectrum has a much narrower hyperfine coupling constant of 58 G while the hyperfine coupling constant of nitrosocyanin is broader at 137, which is typical of type 2 copper sites.[21,27] These spectral differences will be key in using loop directed mutagenesis to identify whether the engineered protein better resembles the scaffold protein or the loop protein.

1.5 LOOP DIRECTED MUTAGENESIS

When comparing cupredoxins we find the copper is typically coordinated by the same equatorial ligands (2His, Cys) found within the active site loop. Three of the 4 coordinating ligands are found within the C-terminal loop.[35] Often the remaining residues of the loop differ between cupredoxins.[36] The cupredoxin active site loop is found between β-strand 7 and β-strand 8, the variance in length between these rigid β-strands may play a role in the different geometry of the active sites and thus spectroscopic differences.

Loop directed mutagenesis is site directed mutagenesis of sequential residues which utilizes an active site loop sequence to replace an existing loop sequence. This method has been studied within various metalloproteins including heme proteins,[37] Fe-S cluster proteins[38] and cupredoxins. Within cupredoxins loop mutagenesis has proven to successfully model a few native loop proteins.[39] Yanagisawa and Dennison studied four loop contraction models,

which replaced a longer loop with a shorter one, and found that three of the four maintained spectroscopic characteristics of the native scaffold protein and not of the loop. The fourth variant, where the nitrite reductase loop was replaced with the amicyanin loop was unstable and additional studies were not performed.

To elaborate on the above studies, the five residue loop from amicyanin was placed in three cupredoxin scaffolds that contain longer loops. The amicyanin loop replaced the existing loop located between rigid β-sheets of each of the cupredoxins. Pseudoazurin, plastocyanin and azurin were each used as scaffolds for the amicyanin loop, and all typically have a 10 residue loop. The active site loops that were modeled in a scaffold protein, bound copper and were redox active.[40] These loop contraction studies always result in a decrease of redox potential.[35] In the pseudoazurin-amicyanin and plastocyanin-amicyanin mutants the spectroscopy remained very similar to WT pseudoazurin and plastocyanin suggesting the scaffold dictates the copper site properties. However the azurin-amicyanin mutant resulted in significant differences in UV-visible and EPR spectra compared to WT azurin and was more similar to WT amicyanin.[39] This suggests that the loop is capable of tuning the redox potential as well as lowering the reorganization energy to better facilitate electron transfer.[41]

Further loop studies, called loop elongation, involved placing a longer loop sequence, like the loop in plastocyanin, into a protein scaffold that typically has a shorter loop, like amicyanin. These experiments resulted in variants with spectroscopic properties that do not necessarily match the native scaffold protein

or the native loop protein. Rather the copper site characteristics were a mix of both the native loop and native scaffold protein properties. This shows that the metal binding loop interaction with the β-sheets of the scaffold can influence the active site geometry.[40]

This method of loop mutagenesis has been used to model other copper binding proteins such as the Cu_A class protein cytochrome c oxidase. The copper binding loop of cytochrome c oxidase was modeled in azurin and found to have a very weak absorption signal and a second mutation within the cytochrome c oxidase loop was performed that mutated a Tyr to a Leu which is like WT azurin. This mutant when binding Cu(II) gave a nice purple color and had UV-visible and EPR spectroscopy similar to WT cytochrome c oxidase.[42-43] In this study the loop also determined the spectroscopic characteristics of the mutant. This is similar to the loop contraction study mentioned above, where the amicyanin loop was placed in the azurin scaffold and the spectroscopic properties of the native loop protein were maintained.[35]

Design of both heme and 4Fe-4S cluster active sites were incorporated into simple synthetic peptides that mimicked ferredoxin. The UV-visible spectra and EPR for these mutants proved to be similar to ferredoxin from *P. aerogenes*. They found the 4Fe-4S clusters were able to generate peptide folding under physiological conditions. This suggests the 4Fe-4S cluster sites plays a significant role in protein structure and thus function.[37]

We have also used this method of loop directed mutagenesis to initially determine whether the nitrosocyanin loop can accurately be modeled in azurin.

Secondly this model has been used to examine the structure-function relationship of nitrosocyanin. This protein has not been identified as a type 1 copper protein or cupredoxin. However with such structural similarities to the cupredoxins, particularly with a similar β-sheet arrangement, we hypothesize this method will allow us to recreate the nitrosocyanin loop in azurin. We are curious whether the spectroscopic characteristics will be similar to Dennison's loop contraction studies where the scaffold protein determined the copper characteristics or like Hay's Cu_A loop design which showed the loop dictated the properties of the copper center.

CHAPTER 2: DESIGN AND SYNTHESIS OF NITROSOCYANIN AZURIN MUTANT

2.1 MUTAGENESIS OF AZURIN TO INCORPORATE NITROSOCYANIN LOOP

The gene for *Pseudomonas aeruginosa* azurin was a generous gift from John H. Richards (California Institute of Technology, Pasadena, CA) and provided by Yi Lu (University of Illinois U.C., Urbana, IL). The azurin gene was subcloned into *Escherichia coli* placing the gene under control of the lac promoter.[23] The pET9a (Novagen) expression vector contained a gene expressing kanamycin resistance. Initially, the nitrosocyanin loop residues were identified using the nitrosocyanin crystal structure (PBD ID:1IBY) and visualizing it with PyMol v0.99. This was compared to the crystal structure of the azurin loop. (PBD ID: 4AZU) The nitrosocyanin loop consisted of 10 residues, ^{96}GlnLeuHisProLysAsnIleHisLeuPro^{105}. This loop replaced residues ^{113}ThrPheProGlyHisSerAlaLeuMetLys^{122} in azurin. These specific mutations in the azurin gene were designed by pDRAW32 1.1.0.106 (freeware ACACLONE software) in primers for loop directed mutagenesis. Primers for the nitrosocyanin loop were 74 base pairs in length and designed to delete an SmaI restriction enzyme site. Using Stratagene quikchange mutagenesis the Loop mutation was incorporated into the azurin gene. Stratagene's quikchange mutagenesis utilized PrimeSTAR polymerase (Takara) as well as the designed primers to incorporate the mutation into copies of the plasmid. The copy DNA was not ligated thus leaving unligated strands. Following quikchange a Dpn1 endonuclease digest

was performed to digest the methylated parent DNA. The nicked copy DNA was then transformed into XL1 Blue *E. coli*. MoBio Laboratories, Inc. miniprep DNA purification of six selected colonies provided DNA that could be digested with the SmaI restriction enzyme. With the deletion of one SmaI site at base pair 4194 the digest identified the loop mutation compared to WT Az. (Fig 8) Then a MoBio Laboratories, Inc. midi prep DNA purification was performed on one selected XL1 Blue *E. coli* colony and sequences were confirmed by UMN Biomedical Genomics center. The Loop DNA was transformed in the BL21* *E. coli* to be used for protein expression and purification.

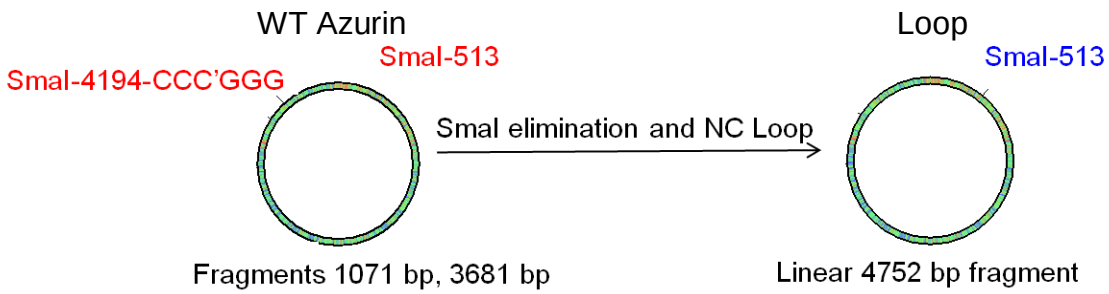

Figure 8 SmaI cut sites in WT Az compared to Az with NC loop incorporated. The loop incorporation deletes the SmaI cut site at basepair 4194. Leaving the single cut site at basepair 513.

2.2 DESIGN OF HIS46 TO GLU MUTATION

An additional mutation was performed in order to complete the copper coordination in the active site of nitrosocyanin. This mutation was His 46 Glu. A second set of complementary primers were designed to incorporate this mutation as well as delete an AclI restriction site. These primers were 43 base pairs. (Fig 9) Through Stratagene Quikchange mutagenesis the His46 to Glu mutation was incorporated into both the wild-type azurin and the Loop mutated sequences to

produce two variants called WTH46E and NCH46E. The sequences were subjected to Dpn1 restriction enzyme digest to destroy the parent DNA. The copy DNA of the wild-type azurin plus His46 Glu (WTH46E) and Loop mutation plus His46 Glu (NCH46E) were individually transformed into XL1 Blue *E. coli.* About 6 colonies from each mutant (WTH46E and NCH46E) were selected and the DNA was purified by mini-prep procedures. (MoBio Laboratories, Inc.) The purified DNA was subjected to AclI restriction enzyme digest to indicate the inclusion of the His46 to Glu point mutation. The DNA was then purified from the best colony of XL1 Blue *E. coli* on a larger scale by midi-prep (MoBio Laboratories, Inc.) for sequencing. The UMN Biomedical Genomics Center confirmed the inclusion of the desired mutations. The DNA was then transformed individually into BL21* *E. coli* cell line and ready for protein expression and purification.

Forward:
5'-CCTGCCGAAGAACGTGATGGGTGAAAACTGGGTTCTGTCCACC-3'
Reverse:
5'-GGTGGACAGAACCCAGTTTTCACCCATCACGTTCTTCGGCAGG-3'

Figure 9 Forward and reverse primer for His46 to Glu mutation. The complementary primers were 43 bp in length.

2.3 HIS46 TO ASP MUTAGENESIS

Another His46 mutation was performed; His46 to Asp. As before, complementary primers were designed. (Fig 10) For this mutation the primers removed a Btg1 restriction site and were 57 base pairs in length. (Fig 11) This mutation was incorporated into both the WT azurin sequence and into the Loop mutated sequence making variants WTH46D and NCH46D, respectively. Following Stratagene Quikchange mutagenesis the parent DNA was digested with Dpn1 restriction enzyme leaving intact copy DNA which was then transformed into XL1 Blue *E. coli*. A mini-prep DNA purification was performed. The isolated DNA, with the correct plasmid variant, was digested with Btg1 restriction enzyme to identify transformants with the correct variant plamid. A midi-prep DNA purification was then performed to gain enough DNA for sequencing at the UMN Biomedical Genomics Center. The sequences were confirmed and the WTH46D and NCH46D sequences were transformed into BL21* *E. coli* for protein expression and purification.

Forward:

5'-
CCGAAGAACGTTATGGGTGATAACTGGGTTCTGTCCACTGCGGCTGACATG
CAAGGC-3'

Reverse:

5'-
GCCTTGCATGTCAGCCGCCGTGGACAGAACCCAGTTTCACCCATAACGTTC
TTCGG-3'

Figure 10 Forward and reverse primers for His46 to Asp mutation. These complementary primers were 57 bp in length. Incorporating this sequence deleted a Btg1 restriction enzyme site at basepair 4005.

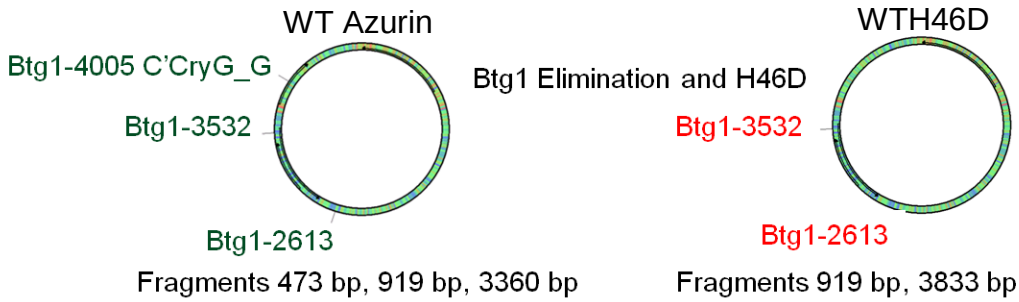

Figure 11 His46 to Asp mutation and Btg1 elimination. The incorporation of the primer into the azurin gene deleted the Btg1 restriction site at basepair 4005.

2.4 PROTEIN EXPRESSION AND PURIFICATION

Protein expression and purification was performed by first growing cells in LB broth (10 g tryptone, 5 g yeast and 10 g NaCl) with kanamycin for 8 h. These cultures were used to inoculate 4 L of 2x YT (20 g NaCl, 40 g yeast and 64 g tryptone) media with kanamycin which grew overnight for about 13 h at 30° C until reaching an optical density at 600 nm of 1.5 or greater. At this point IPTG was added to the cells, which mimics lactose and induces the lac promoter and thus initiates RNA polymerase over production that transcribes azurin or the azurin mutant of interest. The cells continued expressing protein for an additional 3 h when the cells were isolated by centrifugation, 6500 rpm at 4° C for 10 min. The cells were resuspended in a 20% sucrose solution (20% sucrose, 1 mM EDTA, 30 mM Tris at pH 8.0) which permeates the cell wall. Enlarged cells were then lysed by osmotic shock with Millipore water releasing the periplasmic proteins. This method of cell lysis was chosen because of its capability to effectively break the cell wall and leave the plasma membrane intact, as opposed to other lysis methods like French press or sonication.[44-46] Protein precipitation with 500 mM

sodium acetate pH 4.1 removed extraneous proteins by precipitation as well as decreased solution pH essential for further purification. Sequential ionic exchange chromatography was used to further purify azurin and the azurin mutants. Cationic exchange was used first where the protein binds at pH 4.1 and the protein was eluted with 50 mM ammonium acetate buffer pH 6.35. The cation exchange column was composed of SP-sepharose resin which has negatively charged sulfonyl groups. This was followed by anionic exchange chromatography using the positively charged amine resin, Q-sepharose. The column was equilibrated with the 50 mM ammonium acetate buffer pH 6.35. The protein does not bind to the resin while impurities are bound when it was loaded on the column and immediately eluted. The column was then washed with additional 50 mM ammonium acetate pH 6.35 resulting in the purified protein.

The purified apo protein was detected with absorption spectroscopy, measuring the intensity at 280 nm and using a molar absorptivity of 8440 $M^{-1}cm^{-1}$ to estimate protein concentration and determine 1 equivalent of copper. As the copper was titrated into the azurin active site, copper coordination was detected at 625 nm and 5000 $M^{-1}cm^{-1}$ molar absorptivity was used to determine protein yield. WTH46D mutant was also detected at 625 nm with a molar absorptivity ~4000 $M^{-1}cm^{-1}$ while the Loop mutant and NCH46D were measured at 410 nm with about 4000 $M^{-1}cm^{-1}$ molar absorptivity. Protein identification and purity was also confirmed by SDS-PAGE.

2.5 PREPARING EPR SAMPLES AND DETERMINING ABSORPTIVITY

Each EPR sample was prepared in a specified buffer; 50 mM ammonium acetate pH 5.1 or 6.35, 50 mM phosphate pH 7.0 or 20 mM tris(hydroxymethyl) aminomethane (tris) pH 7.0. The samples were each about 1 mM in buffer and 50% glycerol, and then flash-frozen. The samples were run on a Varian E-line Century Series, X-band EPR instrument at a frequency of 9.27 GHz, perpendicular to the magnetic field. In order to determine the molar absorptivity a 1 mM WT azurin sample was prepared in Tris buffer. This sample and the mutant sample, also in Tris, were run at the same gain of 4000 on the previously mentioned X-band EPR instrument. The area under the curve of the EPR signals was directly proportional to the sample concentration. Using a 1 mM WT Az solution, its absorbance at 625 nm and the mutant's absorbance at 410 nm we were able to determine the molar absorptivity at 410 nm for the mutant protein using Beer-Lambert's Law $A=bC\varepsilon$. Determining a molar absorptivity allowed for more accurate determination of protein concentration and yield.

CHAPTER 3: PROTEIN CHARACTERIZATION

3.1 INTRODUCTION

In this chapter we will present the details of the successful incorporation of the loop mutation into azurin. The complete copper coordination of the nitrosocyanin active site will also be described. These mutations have first been confirmed with restriction enzyme digest and DNA sequencing. Expression and purification of the proteins that bind copper in the active site has also been established and characterized through UV/visible absorption spectroscopy and EPR spectrometry. Finally, the fourth ligand coordinating the copper in nitrosocyanin was introduced in the His46 to Glu mutation. We were unable to express the His46 to Glu mutation in the loop mutant. Following protein purification little absorbance at 280 nm was seen and upon copper titration no Cys(S)→Cu(II) charge transfer bands were observed. The expression problems lead to the design of the His46 to Asp mutation. This mutation maintained the fourth ligand's carboxylate side chain but shortened the group providing more space in the active site for copper coordination.

3.2 MUTAGENESIS RESULTS

3.2.1 LOOP MUTAGENESIS

The nitrosocyanin loop sequence and deleting an SmaI restriction site were successfully incorporated into azurin. The SmaI restriction enzyme cut the 4752 bp plasmid containing the WT Az gene two times, at 4194 bp and 513 bp

resulting in fragments of 3681 bp and 1071 bp. The digests were run on a 1% agarose gel. (Fig 13) Plasmids containing the loop mutation, Loop and NCH46D, were cut once at 513 bp leaving the 4752 bp plasmid as a linear DNA strand. The SmaI digest was also performed on the plasmid containing the WTH46D mutation to demonstrate that the loop was not incorporated as well. The agarose gel of an SmaI restriction digest confirms the expected cut patterns in WT Az, Loop, WTH46D and NCH46D. The plasmid sequence for loop and NCH46D were also determined by UMN Biomedical Genomics Center and found to contain the correct mutation as well as the azurin gene.

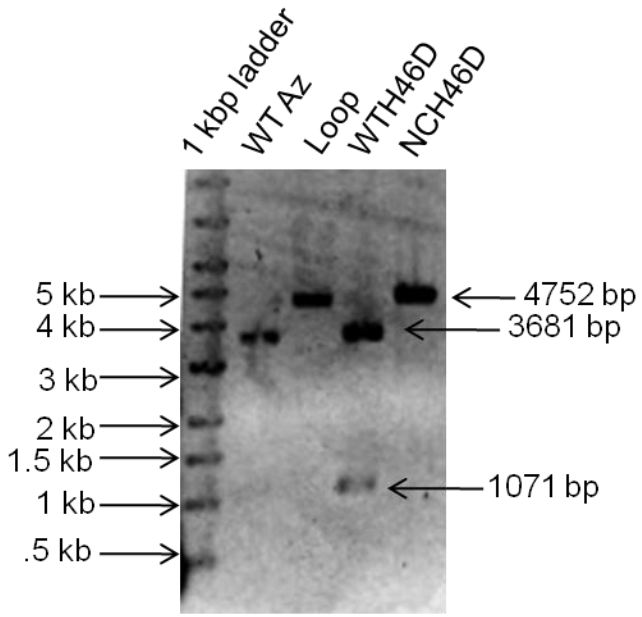

Figure 12 1% agarose gel of SmaI restriction digest. L to R: 1 kb ladder, WT Az, Loop, WTH46D, NCH46D. The SmaI digest cut the WT Az twice leaving two fragments 3681 bp and 1071 bp, respectively. The loop incorporation deleted an SmaI site. After SmaI digest of Loop and NCH46D the DNA was cut once leaving linear DNA strands.

3.2.2 HIS46 TO GLU MUTAGENESIS

The point mutation His46 to Glu was incorporated, by previous students, into both WT Az and the Loop mutant. This mutation was confirmed by Acl1 restriction enzyme digest followed by gel electrophoresis and found to be correct. Sequencing by UMN Biomedical Genomics Center determined the mutation was correctly incorporated into the plasmid containing both WT Az gene and the loop mutation.

3.2.3 HIS46 TO ASP MUTAGENESIS

A final point mutation of His46 to Asp was performed, which also deleted a Btg1 restriction enzyme cut site. The restriction enzyme digest of DNA plasmids containing WT Az or the Loop mutation cut at three sites resulting in three fragments of 3360, 919 and 473 bp, respectively. Restriction digest of NCH46D and WTH46D resulted in two cut sites and two fragments of 3833 bp and 919 bp. (Fig 14) Gel electrophoresis of the Btg1 restriction digest confirmed the expected cut patterns in WT Az, Loop and NCH46D. The gel also confirmed the same cut patterns in WTH46D. (Fig 14) The plasmid sequence for NCH46D was also determined by UMN Biomedical Genomics Center and found to contain the His46 to Asp and loop mutations as well as the azurin gene.

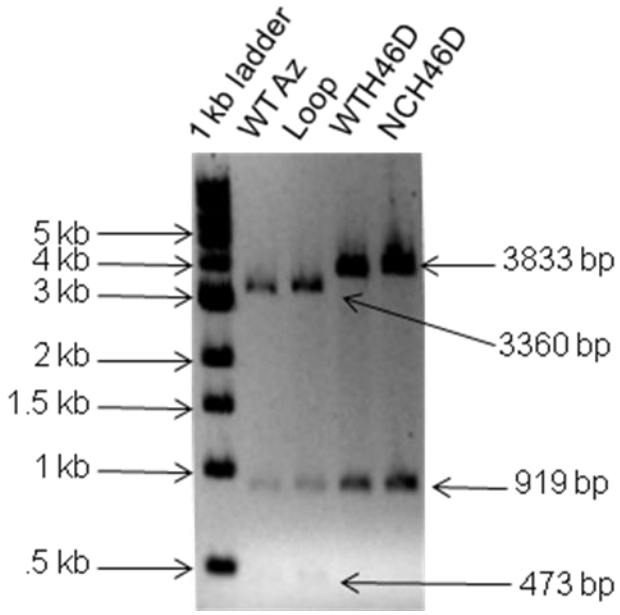

Figure 13 1% agarose gel of Btg1 restriction digest. L to R: 1 kb ladder, WT Az, Loop, NCH46D. The Btg1 digest cut the WT Az and Loop containing plasmids three times resulting in three DNA fragments of 3360 bp, 919 bp and 473 bp respectively. The H46D mutation also deleted a Btg1 site resulting in two cut sites of 3833 bp and 919 bp respectively.

3.3 PROTEIN PURIFICATION RESULTS

Following protein purification of azurin and each azurin mutant, loop, WTH46D and NCH46D, we were able to quantify the protein yield through Cu(II) titration. Each mutant resulted in varying yields. Protein yields were calculated based on the absorbance at 625 nm (5000 $M^{-1}cm^{-1}$)[21] for WT Az and WTH46D, and the absorbance at 410 nm (4000 $M^{-1}cm^{-1}$)[27-28] for the Loop and NCH46D. WT azurin and WTH46D had the best yields of ~75 mg/L of media and ~15 mg/L of media respectively. The loop and NCH46D mutants, which had multiple mutations typically resulted in much lower yields of <5 mg/L of media and <2 mg/L of media. (Table 1) The WTH46E mutation resulted in yields <36 mg/L of media. However, the mutation which incorporated the native nitrosocyanin active

site, NCH46E, has not been isolated suggesting expression problems. This was concluded because UV-visible spectroscopy, following purification, showed negligible absorbance at 280 and no Cys(S)→Cu(II) charge transfer band upon copper titration. SDS-PAGE supported this conclusion and did not exhibit the expected protein band at 14 kDa. These results lead to the development of the His46 to Asp mutation.

Table 1 Protein yields of WT Az, WTH46D, Loop and NCH46D. Each yield was from a 4 L growth.

	Growth 1	Growth 2	Growth 3	Growth 4	
	OD/yield(mg)	OD/yield(mg)	OD/yield(mg)	OD/yield(mg)	Avg
WT Az	1.66/ 300				1.66/300
WTH46D	1.85/ 59				1.85/59
Loop	1.80/ 20	1.86/ 5.5	1.84/ 18	1.93/ 13	1.86/14
NCH46D	1.58/ 2.3	3.07/ 2.3	4.07/ 2.9	3.80/ 11.7	3.13/4.8

12% SDS PAGE gel of a Loop protein purification was run at 200V for 1 hr to confirm the presence of protein throughout the purification steps. The molecular weight of the loop mutant and azurin are similar enough that the bands adjacent to WT Az are likely to be the purified loop. This is consistent with the Cu titration and observed presence of the copper bound protein. Throughout the purification protein with a molecular weight similar to azurin, 14 kDa[8], is present. (Fig 15) This was compared to the sample in lane 2, Empty BL21* cells, which does not contain the azurin gene and thus does not have a band at 14 kDa. A similar gel with samples from an NCH46D growth has not been achieved with acceptable quality and conclusive results to support the acquired spectroscopy.

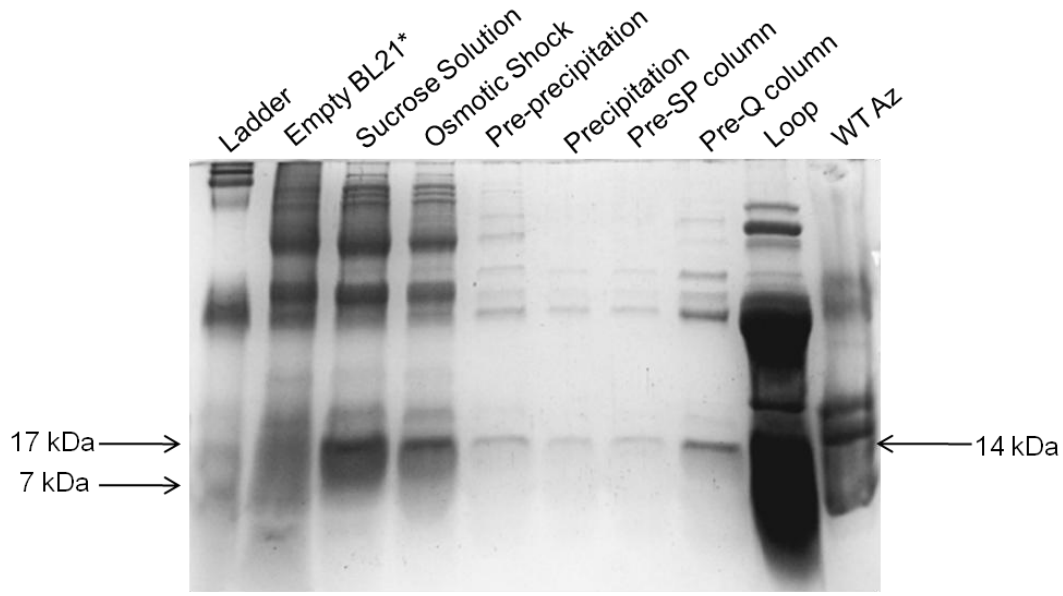

Figure 14 12% SDS PAGE results of Loop purification. Compared protein in BL21* Empty cells to the protein in each step of the purification and finally compared with WT Az. The Loop, like WT Az has a protein band around 14 kDa, which is assumed to be azurin or azurin mutant.

3.4 UV-VISIBLE SPECTROSCOPY

3.4.1 LOOP ABSORPTION SPECTROSCOPY

The loop absorption spectrum is significantly different from WT Az, with peaks at 410, 540 and 720 nm, respectively. Native nitrosocyanin has charge transfer bands at 390, 540 and 720 nm, respectively.[27-28] Similar to native nitrosocyanin the Cys(S)σ→Cu(II) charge transfer band at 410 nm is more intense than the Cys(S)π→Cu(II) charge transfer band at 540 nm. (Fig 16) This suggests a more tetragonally distorted geometry that is more similar to native nitrosocyanin than to the WT Az scaffold.

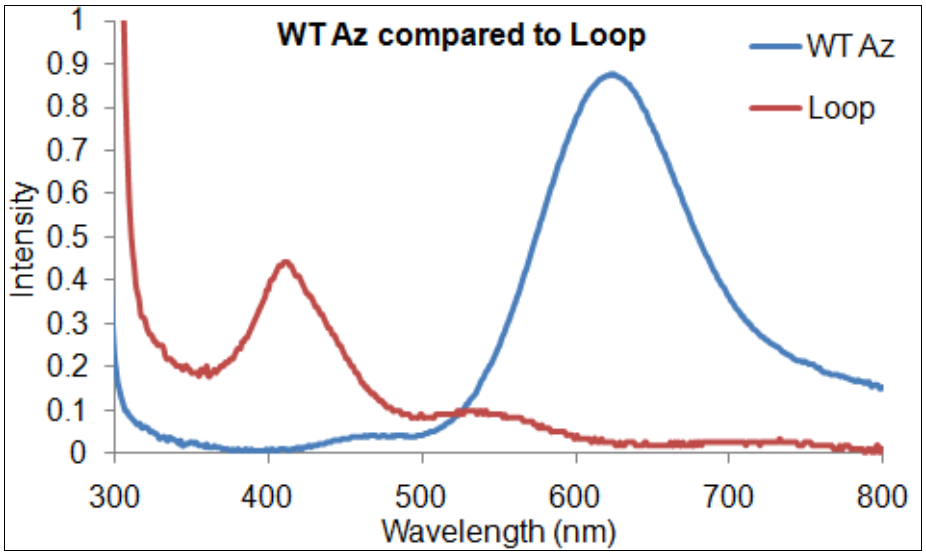

Figure 15 WT Az and Loop mutant UV-visible absorption spectra overlay. These spectra are quite different in that loop looks very similar to native nitrosocyanin in that it has a strong charge transfer band at 410 nm and two smaller charge transfer bands at 540 nm and ~725 nm.

3.4.2 His46 to Glu ABSORPTION SPECTROSCOPY

Initially, the model was designed to incorporate the nitrosocyanin loop mutation, which included the Cys and two His ligands, and finally the Glu ligand was introduced. The final protein, NCH46E, has had expression problems that we are still investigating. NCH46E was not expressed and thus the characteristic spectroscopy of copper binding in the designed active site was not observed. This led us to the design of NCH46D. Asp has the same chemical properties as the Glu in NCH46E but with a shorter side chain.

3.4.3 WTH46D ABSORPTION SPECTROSCOPY

The UV-visible absorption spectrum WTH46D is very similar to WT Az. The Cys(S)π→Cu(II) charge transfer band at 625 nm in WTH46D is similar to that found in WT Az. In addition to the 625 nm absorption the WTH46D

spectrum shows a Cys(S)σ→Cu(II) charge transfer band ~460 nm which is more intense than the Cys(S)σ→Cu(II) in WT Az at ~470 nm. (Fig 17) This suggests the S-Cu bond is slightly distorted compared to that found in WT azurin.

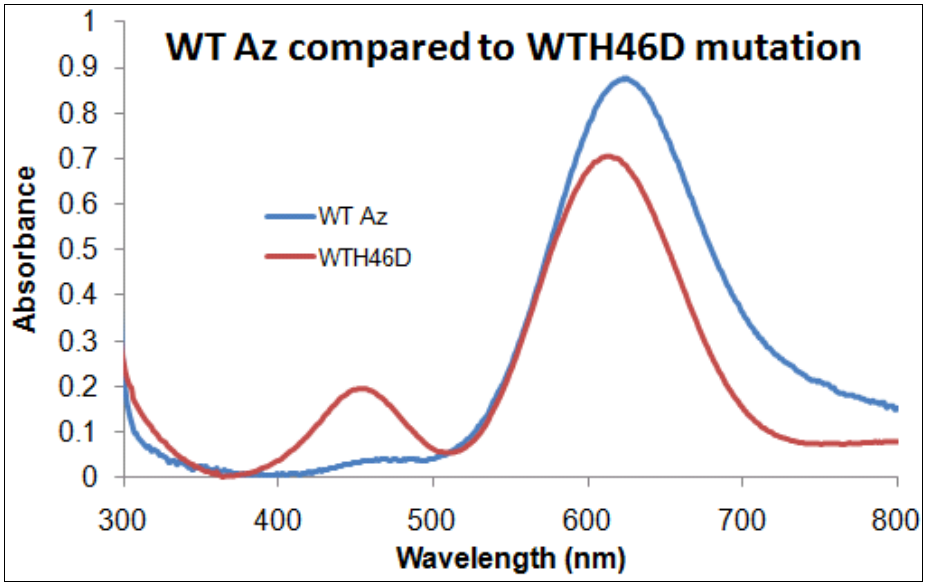

Figure 16 WT Az and WTH46D UV-visible absorption spectra overlay. Both have the intense charge transfer band at 625 nm but WTH46D has an additional band at ~460 nm.

3.4.4 NCH46D ABSORPTION SPECTROSCOPY

Finally, we compared the UV-visible spectrum of NCH46D to the Loop mutant. (Fig 17) This spectrum shares characteristics with the spectrum of native nitrosocyanin and also WT Az. NCH46D has charge transfer bands at 410 nm and 625 nm. This seems to combine the intense Cys(S)π→Cu(II) charge transfer band of the loop and the intense Cys(S)σ→Cu(II) charge transfer band of WT Az. The full nitrosocyanin active site mutant does not spectroscopically model native nitrosocyanin. It appears that the loop itself best models the nitrosocyanin spectrum.

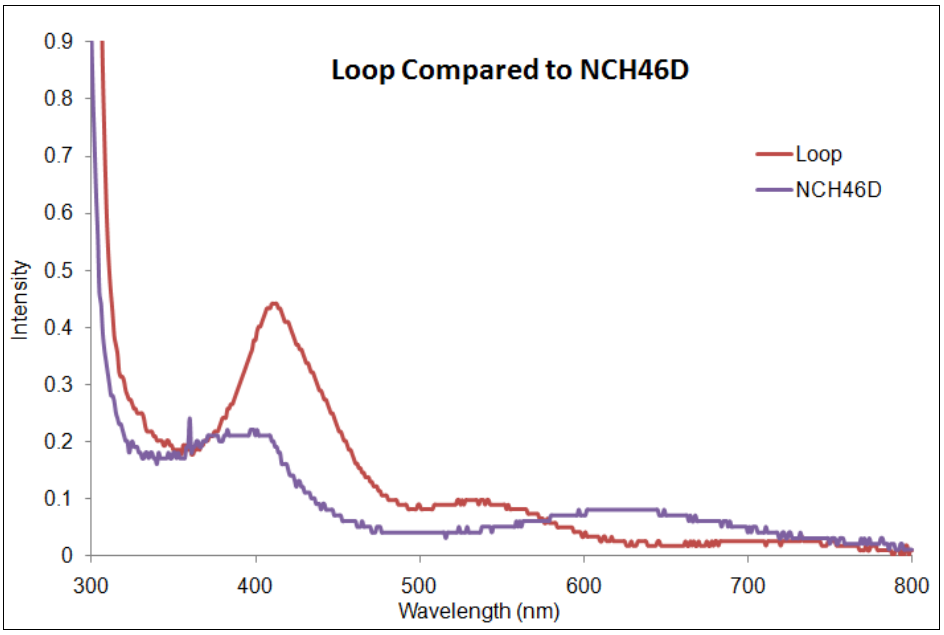

Figure 17 NCH46D compared to Loop UV/visible spectra. The full mutant NCH46D spectrum is significantly different from the loop mutation. NCH46D has a charge transfer band at 410 nm and another charge transfer band at 625 nm. Compared to the loops charge transfer bands at 410, 540 and 720 nm respectively.

3.5 EPR SPECTROMETRY AND DETERMINING MOLAR ABSORPTIVITY

EPR spectroscopy of the H46D and loop mutants each show significant differences from the WT Az spectrum. (Fig 18) Each spectrum shows a single copper species and distinct axial (g_x and g_y) and equatorial ($g_{//}$) regions. The $g_{//}$ region of each spectrum has nice hyperfine splitting which indicates an unpaired electron on the Cu(II) ion. Like all cupredoxins WT Az has a narrow hyperfine region (58 G) while the loop and NCH46D has much broader hyperfine coupling of 166 G and 174 G respectively. (Table 2) These broader hyperfine regions are characteristic of type 2 copper binding proteins and suggest decreasing covalency between Cys(S) and Cu(II). The WTH46D spectrum has unexpected

hyperfines in the g_x and g_y region and lacks hyperfines in the g_z region. This suggests a change in geometry of the Cu active site.

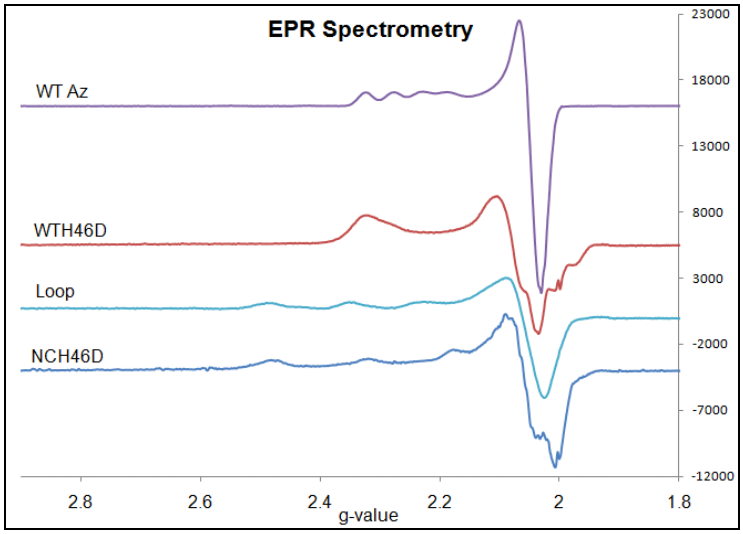

Figure 18 EPR spectra of WT Az, Loop, WTH46D and NCH46D. The hyperfine coupling of Loop and NCH46D is very similar and much larger than WT Az.

Table 2 Reports $g_{//}$ and $A_{//}$ values of WT Az, native nitrosocyanin, WTH46D, Loop and NCH46D.

	$g_{//}$	$A_{//}$ (G)
Native NC[27]	2.25	137
WT Azurin	2.28	58
WTH46D	2.42	150
Loop	2.36	166
NCH46D	2.40	174

EPR spectroscopy was also used to estimate a molar absorptivity for the loop mutant. Based on the direct proportion of the area under the curve to concentration we found the molar absorptivity of the loop mutant to be ~4000 $M^{-1}cm^{-1}$, which is quite similar to azurin's molar absorptivity at 625 nm (~5000 $M^{-1}cm^{-1}$)[21] but smaller than the molar absorptivity of native nitrosocyanin at 390 nm (7000 $M^{-1}cm^{-1}$).[28] (Fig 19) Determining the molar absorptivity of the loop mutant allowed for more accurate yield calculations.

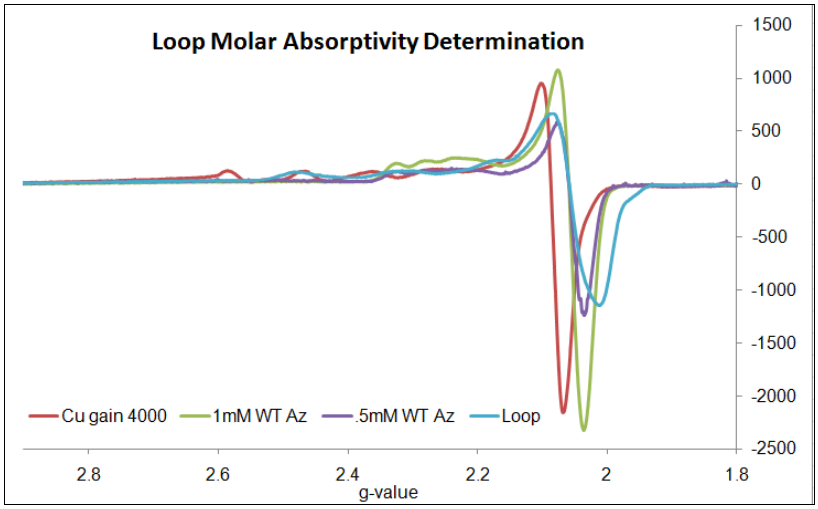

Figure 19 Loop, 1 mM Cu(II), 1 mM WT Az and 0.5 mM WT Az spectra to determine Loop molar absorptivity. Estimation for loop molar absorptivity was determined to be ~4000 $M^{-1}cm^{-1}$.

CHAPTER 4: ACTIVITY ASSAYS

4.1 ACTIVITY ASSAYS FOR NITROSOCYANIN

Nitrosomonas europaea's use of ammonia, carbon dioxide and mineral salts for energy and survival have made the bacterium a point of interest in the current energy crisis. Many enzymes with leading roles in nitrogen metabolism have been elucidated in this bacterium. The unusual red color of nitrosocyanin suggests the protein may function differently from the typical type 1 blue copper protein. Although nitrosocyanin has been crystallized and spectroscopically characterized, the function has not been elucidated. Nitrosocyanin is found in concentrations equivalent to ammonia oxidizing enzymes and thus may also be involved in this metabolic system. Through genomic sequencing genes and thus proteins have been identified and their homologues in other species have suggested probable functions.[47] Determining the function of this enzyme may lead to improved design of industrial catalysts and a better understanding of the metalloprotein's structural and functional relationships.

The open binding site in nitrosocyanin's active site suggests it may be a type 2 copper binding protein. Based on the variety of catalytic functions found in type 2 copper proteins we hope these will lead to elucidating the function of nitrosocyanin and thus classifying the protein as a type 2 copper protein. There is a number of type 2 copper binding proteins found to have nitrite reductase activity, superoxide dismutase (SOD) or oxygenase activity. We will begin by probing nitrosocyanin for superoxide dismutase activity and further exploring

other enzyme activities. The nitrosocyanin active site is structurally similar to native SOD enzymes. Other interesting assays would be nitrite reductase and nitric oxide reductase assays. Both activities are necessary for *N. europaea* survival to prevent accumulation of toxic nitrite.[33]

4.2 SOD ACTIVITY ASSAY

Superoxide was found to be a toxic oxygen species only produced in respiring cells. This was concluded because all cells that underwent aerobic respiration contained superoxide dismutase enzymes. There are a variety of SOD enzymes ranging from Cu-Zn species, Mn species as well as Fe containing SODs, all with the same underlying activity but with different structural characteristics. Nitrosocyanin has a relatively similar active site coordination and substrate binding pocket, to that of Mn-SOD.[48-49] SOD catalyzes the dismutation of superoxide producing molecular oxygen and peroxide.

$$O_2^{\cdot -} + O_2^{\cdot -} + 2H^+ \rightarrow O_2 + H_2O_2$$

A superoxide dismutase assay was developed by Fridovich and McCord in 1969 when studying erythrocuprein, also known as Cu/Zn-SOD. In this assay they used xanthine and excess molecular oxygen and water to generate superoxide in the presence of xanthine oxidase. Superoxide production was directly proportional to urate production. Urate, the product of xanthine oxidation, can be monitored by absorption spectroscopy at 290 nm.[50-51] Oxidized cytochrome c (cyt c) was used to measure the oxidation of the superoxide radical. This reduction of cyt c is measured with absorption spectroscopy at 550

nm. (Fig 20) When SOD was present, however, the cyt c and SOD compete for the generated superoxide radical. (Fig 21) The SOD would have a higher affinity for the radical and thus cyt c reduction would not occur to the same extent and the SOD activity could be quantified.[52]

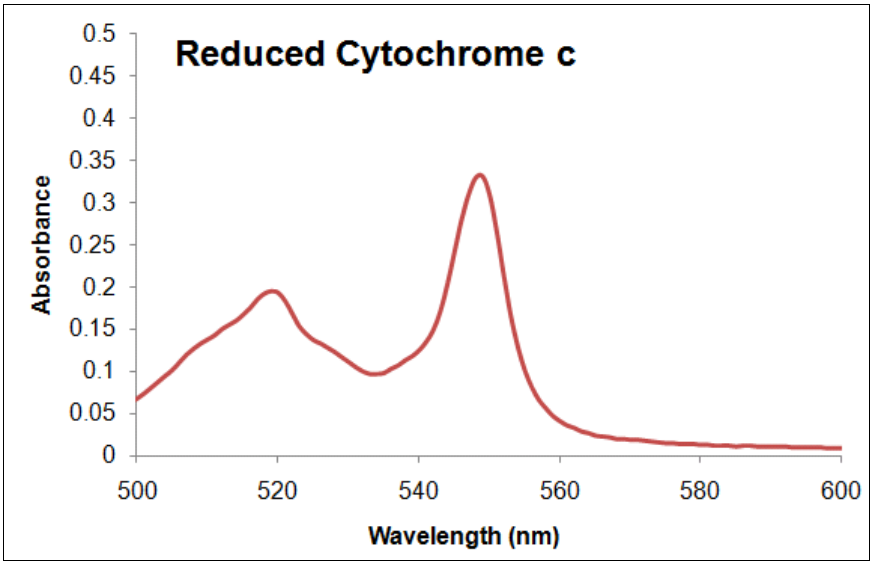

Figure 20 Fully reduced cytochrome c. Reduction of cytochrome c can be measured at 550 nm. In the SOD activity assay cytochrome c reduction would suggest the SOD enzyme has little activity.

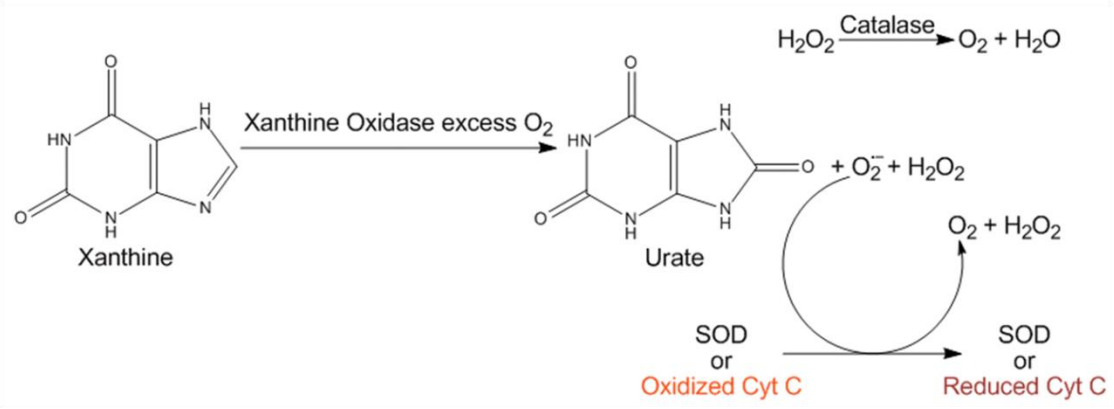

Figure 21 Superoxide dismutase reaction scheme. Xanthine is oxidized by xanthine oxidase in the presence of excess oxygen to form urate, superoxide and hydrogen peroxide. The superoxide radical can then be oxidized by cyt c or dismutated by SOD to form molecular oxygen and peroxide.

We chose this assay because it is common to test copper for SOD activity and because it is a simple step in determining the catalytic function of nitrosocyanin. A number of groups have been interested in developing small molecule copper complexes that mimic SOD activity. For example three Cu complexes of nicotinic acid-2-hydroxypyridine, nicotinic acid-s-aminopyridine and nicotinic acid-picolinic acid were found to have some SOD activity.[53] And many other Cu containing compounds have been successfully determined to mimic SOD activity, such as 2,2-dimethylpentanedioic acid, (benzoicacid)2(bipy)(H_2O), and (salicylic acid)2(benzimidazole)2.[54-55] Each apo-complex was also assayed and found to have negligible activity. This suggests that the Cu ion is important in providing the complexes with SOD activity and likely significant in copper binding enzymes expressing SOD activity.[53]

4.3 SOD ASSAY EXPERIMENTAL DETAILS

Native SOD was obtained from Sigma Aldrich and xanthine oxidase (XO) from Sigma Aldrich and Calibiochem. Nitrosocyanin proved to be more stable at physiological pH, thus 20 μM Tris buffer pH 7.0 was used to prepare all reagents. A 3 mL quartz cuvette was used as the reaction chamber. Under constant stirring, reagents were added specifically in the following order; Tris buffer followed by 10 μM oxidized cyt c. Initially, these were measured with UV-visible absorption spectroscopy to ensure full oxidation of cyt c (410 nm). The xanthine prepared in tris buffer pH 7.0 was then added for a final concentration of 50 μM and absorption at 270 nm was observed, characteristic of xanthine. Finally, in

the specified order the following enzymes were added 2.12 units of catalase, 20 μM SOD or azurin mutant of interest and finally 0.05 units of xanthine oxidase. (Table 3)

Table 3 SOD Assay reagents and the specific order and concentration following the method of Fridovich and McCord from 1969.

Reagent Order	Reagent Final Concentration	Volume
Tris Buffer pH 7.0	20 mM	1186.6 μL
120 μM Oxidized Cytochrome C	10 μM	250 μL
100 μM Xanthine	50 μM	1500 μL
630 μg/mL Catalase	20 μg	32 μL
2 mM SOD or azurin mutant	2.12 units	29 μL
62.5 units Xanthine oxidase	0.05 units	2.4 μL
TOTAL		3000 μL

Initially, a control was performed as described above, without SOD or the azurin mutant of interest. This was called the negative control. A positive control was also performed which contained the native SOD enzyme. The azurin and mutant azurin species (Loop, WTH46D, and NCH46D) were then assayed at concentrations of 20 μM and 10 μM. The overall change in absorption at 550 nm over time was compared between the controls and each assay with azurin or azurin mutant. A small change over time suggested higher SOD activity.

4.4 SOD RESULTS

The SOD activity assay proved more intricate than expected. The original xanthine oxidase, from Sigma Aldrich proved to be unstable. Enzyme purchased from Calibiochem was used and achieved consistent results. Upon using a concentration of 0.05 U per assay, the xanthine oxidase generated appropriate

and consistent levels of superoxide. With high levels of superoxide produced cyt c was fully reduced showing a significant Δ550 nm > 0.15. (Fig 22) This is greater than the change seen by McCord and Fridovich in 1969.[52] The Δ550 nm for the positive control using native Cu/Zn-SOD was ~0.011 which is nearly a ten-fold decrease in superoxide concentration. The assay with $CuSO_4$ as a catalyst showed the SOD activity found in free copper. This was used as a control in order to determine if activity seen in the azurin and azurin mutant assays was a result of free Cu(II) ions or rather the copper bound protein itself. Free copper showed a change of ~0.016 at 550 nm, which is comparable to native Cu/Zn-SOD. The assay with WT Az shows activity most similar to SOD with ~0.030 Δ550 nm. (Fig 22) This was unexpected because WT Az is a well known electron transfer protein.[8] Therefore, azurin's function can also suggest that the superoxide radical may be donating the unpaired electron to the Cu(II) active site and reducing it to Cu(I), just as cyt c is reduced from Fe(III) to Fe(II). This would prevent the reduction of cyt c in the assay and results might therefore resemble the native SOD. Also seen in the azurin assay is the decreasing charge transfer band at 625 nm as the 550 nm band increases. (Fig 23) This suggests Cu(II) reduction to Cu(I).

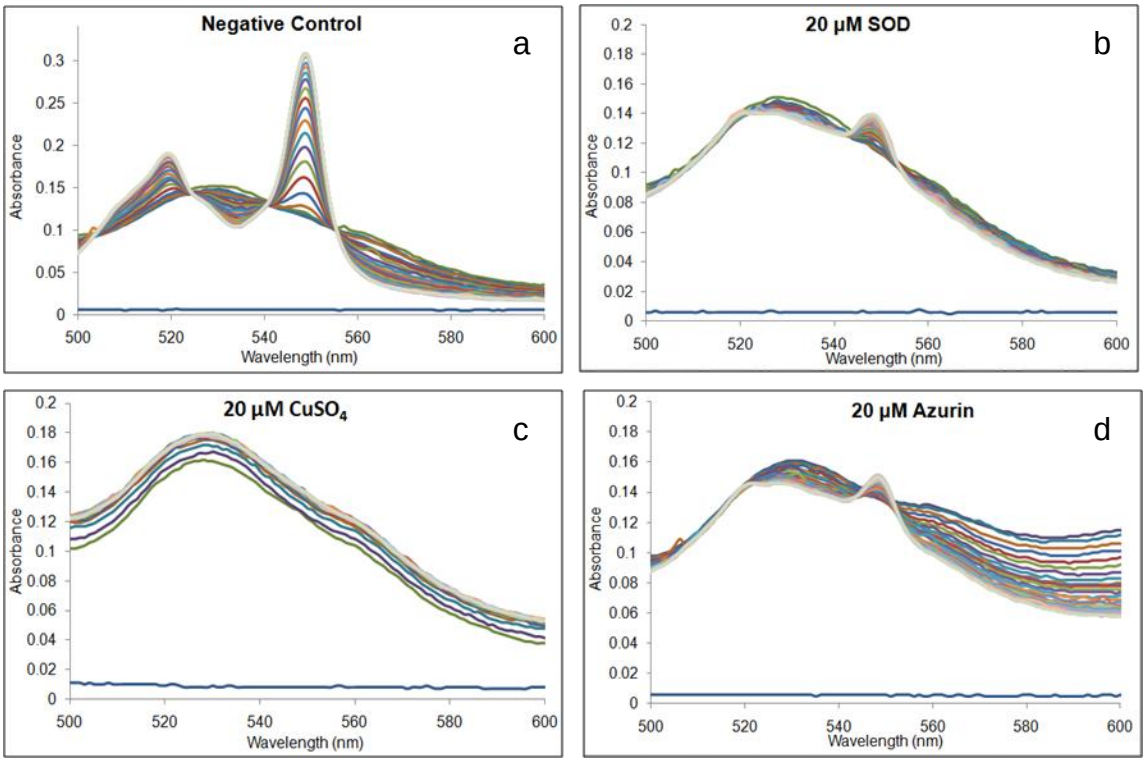

Figure 22 Negative Control (a), Positive Control (b), $CuSO_4$ (c) and Azurin (d) SOD assays. The results show the difference between no SOD activity in the negative control and native SOD activity in the positive control. The $CuSO_4$ and Azurin assays show results similar to that of SOD activity that show underlying SOD activity in Cu(II) molecules.

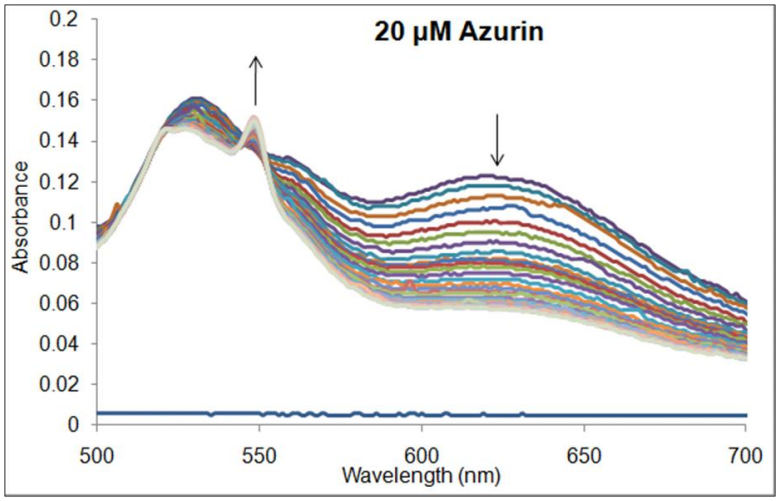

Figure 23 WT Az SOD assay. Over time as the cyt c is being reduced the Cys(S)→Cu(II) charge transfer band at 625 nm is decreasing.

With the H46D mutations we are able to see results similar to native SOD, azurin and free copper. In the presence of 6.67 μM of NCH46D we see no change in absorbance at 550 nm, and with 3.33 μM NCH46D there is only a 0.040 change. (Fig 25) We can assume 50 μM superoxide was produced from the 50 μM xanthine and xanthine oxidase. Thus, the assay contained 50 μM superoxide, 20 μM cyt c and significantly lower NCH46D concentrations of 3.33 μM and 6.67 μM. If simple reduction of the azurin were occurring without superoxide dismutation, we would still expect to see reduction of the cyt c after the small concentration of NCH46D was reduced to Cu(I). However, in the presence of this excess superoxide only a small amount of cyt c reduction occurs. This suggests that NCH46D has SOD activity and the enzyme can catalyze the dismutation of superoxide.

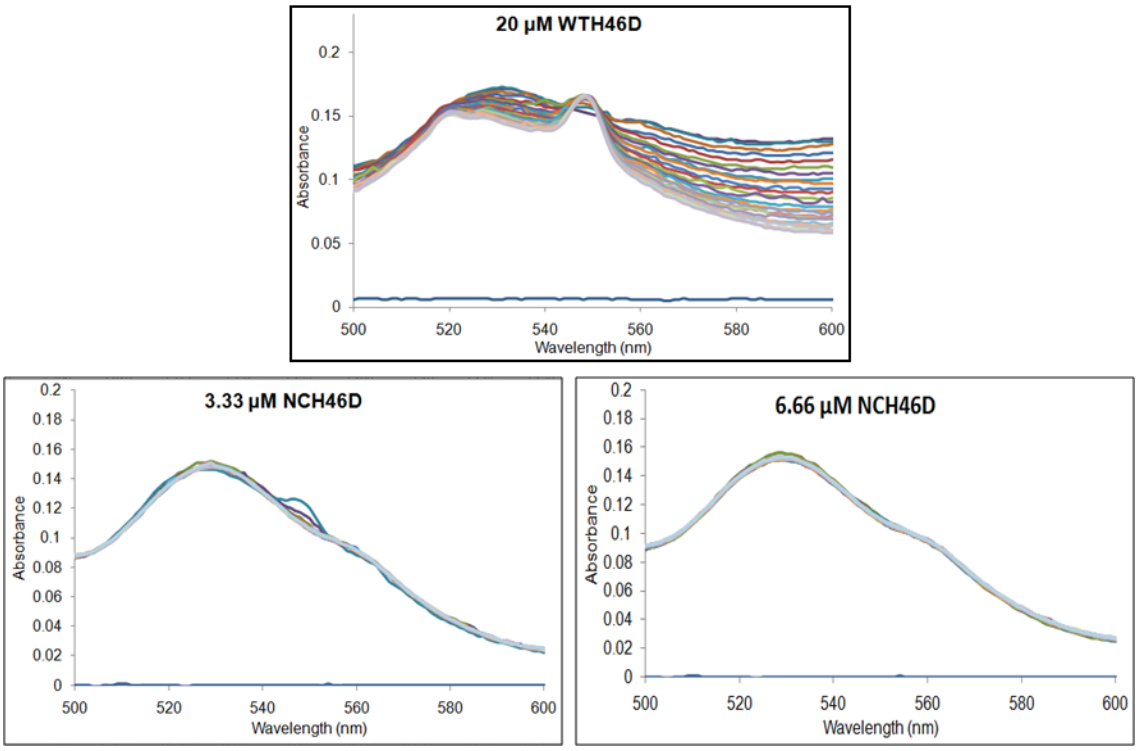

Figure 24 H46D mutant SOD Assays. WTH46D results are similar to WT Azurin while both concentrations of NCH46D are comparative to results seen with the $CuSO_4$ SOD assay.

In order to determine whether the SOD-like activity seen in azurin and the mutants is SOD activity and not oxidation of the superoxide radical additional assays should be performed. Confirming the production of peroxide, a product of superoxide dismutation, would suggest SOD activity. (Fig 22) The SOD activity assay showed the negative control was able to generate superoxide by the intense Δ550 nm. This was used to compare Cu/Zn-SOD, WT Az, Cu(II) and the full mutant NCH46D. We are able to see the difference in cyt c reduction between each of the four compared to the negative control. (Fig 25)

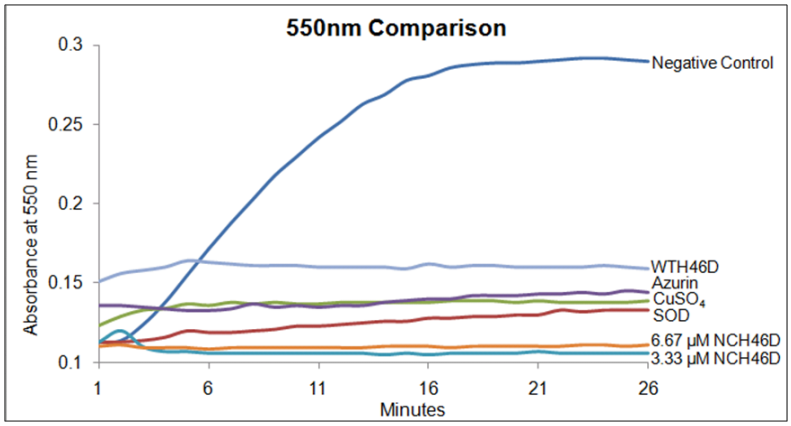

Figure 25 Comparison at Δ550 nm of negative and positive controls, Cu(II), Cu/Zn-SOD, WTH46D and NCH46D. This shows the significant difference between the negative control and the other assays.

Finally, the rate of superoxide degradation was estimated with the negative control, Cu(II), native SOD, WTH46D and NCH46D at 3.33 µM and 6.67 µM. We determined the change in absorbance at 550 nm over time, giving a slope. The slope was divided by the molar absorptivity of reduced cyt c, 29,500 $M^{-1}cm^{-1}$, [56] giving a rate of superoxide consumption. We found that the negative control had the greatest rate while native SOD, Azurin, NCH46D, $CuSO_4$ and WTH46D all had similar rates of consumption. (Table 4) These preliminary calculations support our conclusion that NCH46D may have SOD activity. Further studies should be performed to determine units of SOD activity.

Table 4 SOD Assay Δ550 nm and rate of superoxide degradation.

	Δ550 nm	Slope (Abs./min)	Rate (μM/min)
Negative Control	0.1610	0.01070	0.3627
Cu/Zn-SOD	0.0210	0.00095	0.0322
$CuSO_4$	0.0160	0.00094	0.0319
Azurin	0.0110	0.00048	0.0163
WTH46D	0.0110	0.00069	0.0239
3.33 μM NCH46D	0.0400	0.02000	0.6780
6.67 μM NCH46D	0.0030	0.00075	0.0254

CHAPTER 5: NATIVE NITROSOCYANIN AND DESIGNED MUTANT COMPARISON

The UV-visible and EPR spectra of the loop and NCH46D mutants suggest that these designed metalloproteins are more similar to type 2 copper proteins, like nitrite reductase.[3] The full mutant, NCH46D, appears to have perturbed UV-visible spectroscopy and does not necessarily identify with that of native nitrosocyanin. NCH46D has a charge transfer band at 410 nm like the loop model and one at 625 nm like WT Az. However, UV-visible spectroscopy of the loop mutant shows a spectrum very similar to the native nitrosocyanin. This suggests that in our loop mutagenesis model the loop sequence is more significant to the spectroscopic characterization than the scaffold protein. This conclusion is similar to the results seen by Hay's Cu_A studies of cytochrome c oxidase.[42] Our EPR data also supports this conclusion due to the hyperfine coupling which is much larger than typical type 1 copper proteins. In the EPR spectrum for NCH46D the super-hyperfine structures seen in the g_x, g_y region indicate a rhombically distorted active site which is different from the scaffold protein, azurin.

Here we report that the full mutant does appear to have SOD activity. However, further studies will be needed to determine the products formed. Also further assays such as nitrite reductase and nitric oxide reductase assays will be attempted to see if nitrosocyanin could be involved in nitrogen metabolism. We have also concluded that in this case the loop is significant to the spectroscopy of the model.

REFERENCES

1. Hsiu, J., E.H. Fischer, and E.A. Stein, *α-Amylases as calcium-metalloenzymes. II. Calcium and the catalytic activity.* Biochemistry, 1964. **3**(1): p. 61-6.
2. Couto, S.R. and M.A. Sanroman, *Application of solid-state fermentation to food industry - a review.* J. Food Eng., 2006. **76**(3): p. 291-302.
3. Lippard, S.J. and J.M. Berg, *Principles of Bioinorganic Chemistry*. 1994, Mill Valley, CA: University Science Books. 411.
4. Yanagisawa, S. and C. Dennison, *Reduction potential tuning at a type 1 copper site does not compromise electron transfer reactivity.* J Am Chem Soc, 2005. **127**(47): p. 16453-9.
5. Buning, C., G.W. Canters, P. Comba, C. Dennison, L. Jeuken, M. Melter, and J. Sanders-Loehr, *Loop-Directed Mutagenesis of the Blue Copper Protein Amicyanin from Paracoccus versutus and Its Effect on the Structure and the Activity of the Type-1 Copper Site.* J. Am. Chem. Soc., 2000. **122**(2): p. 204-211.
6. Dennison, C., *Investigating the structure and function of cupredoxins.* Coordination Chemistry Reviews, 2005. **249**(24): p. 3025-3054.
7. Bertini, I., H.B. Gray, S.J. Lippard, and J.S. Valentine, *Bioinorganic Chemistry*. 1994, Sausalito, CA: University Science Books. 611.
8. Messerschmidt, A., R. Huber, T. Poulos, K. Wieghardt, Editors, and U.R.L. Uk. Field, *Handbook of Metalloproteins, Volume 2*. 2001. 785 pp.

9. Solomon, E.I., *Spectroscopic Methods in Bioinorganic Chemistry: Blue to Green to Red Copper Sites.* Inorg Chem, 2006. **45**(20): p. 8012-8025.

10. Berry, S.M., J.R. Mayers, and N.A. Zehm, *Models of noncoupled dinuclear copper centers in azurin.* JBIC, J. Biol. Inorg. Chem., 2009. **14**(1): p. 143-149.

11. Jaenicke, E. and H. Decker, *Functional changes in the family of type 3 copper proteins during evolution.* ChemBioChem, 2004. **5**(2): p. 163-169.

12. Lu, Y., S.M. Berry, and T.D. Pfister, *Engineering novel metalloproteins: Design of metal-binding sites into native protein scaffolds.* Chemical Reviews (Washington, D. C.), 2001. **101**(10): p. 3047-3080.

13. Iwata, S., *Structure and function of bacterial cytochrome c oxidase.* J. Biochem., 1998. **123**(3): p. 369-375.

14. Kroneck, P.M.H., W.E. Antholine, D.H.W. Kastrau, G. Buse, G.C.M. Steffens, and W.G. Zumft, *Multifrequency EPR evidence for a bimetallic center at the CuA site in cytochrome c oxidase.* FEBS Letters, 1990. **268**(1): p. 274-276.

15. Hay, M.T., *Engineering a Purple CuA Site into the Blue Copper Protein Azurin: Construction, Spectroscopy, and Metal substution Studies*, in *Chemistry*. 1998, University of Illinois at Urbana-Champaign: Urbana. p. 177.

16. Formosinho, S.J. and L.G. Arnaut, *Theory of electron transfer reactions in blue-copper proteins.* Res. Chem. Intermed., 2001. **27**(1-2): p. 103-124.

17. Jeuken, L.J.C. and F.A. Armstrong, *Electrochemical Origin of Hysteresis in the Electron-Transfer Reactions of Adsorbed Proteins: Contrasting Behavior of the \"Blue\" Copper Protein, Azurin, Adsorbed on Pyrolytic Graphite and Modified Gold Electrodes.* J. Phys. Chem. B, 2001. **105**(22): p. 5271-5282.

18. Nar, H., A. Messerschmidt, R. Huber, M. van der Kamp, and G.W. Canters, *Crystal Structure Analysis of Oxidized Pseudomonas aeruginosa Azurin at pH 5.5 and pH 9.0 A pH-induced Conformational Transition Involves a Peptide Bond Flip.* J. Mol. Biol., 1991. **221**: p. 765-772.

19. Adman, E.T., R.E. Stenkamp, L.C. Sieker, and L.H. Jensen, *A Crystallographic Model for Azurin at 3 Å Resolution.* Journal of Molecular Biology, 1978. **123**: p. 35-47.

20. Nar, H., A. Messerschmidt, R. Huber, M. van de Kamp, and G.W. Canters, *Crystal structure of Pseudomonas aeruginosa apo-azurin at 1.85 .ANG. resolution.* FEBS Lett., 1992. **306**(2-3): p. 119-24.

21. Adman, E.T., *Structure and function of small blue copper proteins,* in *Topics in Molecular and Structural Biology: Metalloproteins,* P. Harrison, Editor. 1985, MacMillan: New York. p. 1-42.

22. van de Kamp, M., F.C. Hali, N. Rosato, A.F. Agro, and G.W. Canters, *Purification and characterization of a non-reconstitutable azurin, obtained by heterologous expression of the Pseudomonas aeruginosa azu gene in Escherichia coli.* Biochim Biophys Acta, 1990. **1019**(3): p. 283-92.

23. Chang, T.K., S.A. Iverson, C.G. Rodrigues, C.N. Kiser, A.Y.C. Lew, J.P. Germanas, and J.H. Richards, *Gene Synthesis, Expression, and Mutagenesis Of the Blue Copper Proteins Azurin and Plastocyanin.* Proceedings of the National Academy of Sciences of the United States of America, 1991. **88**(4): p. 1325-1329.

24. Karlsson, B.G., T. Pascher, M. Nordling, R.H.A. Arvidsson, and L.G. Lundberg, *Expression of the blue copper protein azurin from Pseudomonas aeruginosa in Escherichia coli.* FEBS Lett., 1989. **246**(1-2): p. 211-17.

25. Lieberman, R.L., D.M. Arciero, A.B. Hooper, and A.C. Rosenzweig, *Crystal Structure of a Novel Red Copper Protein from Nitrosomonas europaea.* Biochemistry, 2001. **40**(19): p. 5674-5681.

26. Hooper, A.B.a.A., David M., *Characterization of a novel red copper protein from nitrosomonas europaea.* Journal of Inorganic Biochemistry 1999. **74**.

27. Arciero, D., M., B. Pierce, S., M. Hendrich, P., and A. Hooper, B., *Nitrosocyanin, a red cupredoxin-like protein from Nitrosomonas europaea.* Biochemistry, 2002. **41**(6): p. 1703-9.

28. Basumallick, L., R. Sarangi, S. DeBeer George, B. Elmore, A.B. Hooper, B. Hedman, K.O. Hodgson, and E.I. Solomon, *Spectroscopic and Density Functional Studies of the Red Copper Site in Nitrosocyanin: Role of the Protein in Determining Active Site Geometric and Electronic Structure.* Journal of the American Chemical Society, 2005. **127**(10): p. 3531-3544.

29. Whittaker, M., D. Bergmann, D. Arciero, and A.B. Hooper, *Electron transfer during the oxidation of ammonia by the chemolithotrophic bacterium Nitrosomonas europaea.* Biochimica et Biophysica Acta, Bioenergetics, 2000. **1459**(2-3): p. 346-355.

30. Gray, H.B., B.G. Malmström, and R.J.P. Williams, *Copper coordination in blue proteins.* J. Biol. Inorg. Chem., 2000. **5**(5): p. 551-559.

31. Hooper, A.B., D. Arciero, D. Bergmann, and M.P. Hendrich, *The oxidation of ammonia as an energy source in bacteria.* Adv. Photosynth. Respir., 2004. **16**(Respiration in Archaea and Bacteria): p. 121-147.

32. Hooper, A.B., T. Vannelli, D.J. Bergmann, and D.M. Arciero, *Enzymology of the oxidation of ammonia to nitrite by bacteria.* Antonie van Leeuwenhoek, 1997. **71**(1-2): p. 59-67.

33. Arp, D.J., L.A. Sayavedra-Soto, and N.G. Hommes, *Molecular biology and biochemistry of ammonia oxidation by Nitrosomonas europaea.* Archives of Microbiology, 2002. **178**(4): p. 250-255.

34. Solomon, E.I., J.W. Hare, D.M. Dooley, J.H. Dawson, P.J. Stephens, and H.B. Gray, *Spectroscopic Studies of Stellacyanin, Plastocyanin, and Azurin. Electronic Structures of the Blue Copper Sites.* Journal of the American Chemical Society, 1980. **102**(1): p. 168-178.

35. Dennison, C., *Ligand and loop variations at type 1 copper sites: influence on structure and reactivity.* Dalton Trans, 2005(21): p. 3436-42.

36. Li, C., M.J. Banfield, and C. Dennison, *Engineering Copper Sites in Proteins: Loops Confer Native Structures and Properties to Chimeric Cupredoxins.* Journal of the American Chemical Society, 2007. **129**(3): p. 709-718.

37. Gibney, B.R., S.E. Mulholland, F. Rabanal, and P.L. Dutton, *Ferredoxin and ferredoxin-heme maquettes.* Proc. Natl. Acad. Sci. U. S. A., 1996. **93**(26): p. 15041-15046.

38. Mulholland, S.E., B.R. Gibney, F. Rabanal, and P.L. Dutton, *Determination of Nonligand Amino Acids Critical to [4Fe-4S]2+/+ Assembly in Ferredoxin Maquettes.* Biochemistry, 1999. **38**(32): p. 10442-10448.

39. Yanagisawa, S. and C. Dennison, *Loop-Contraction Mutagenesis of Type 1 Copper Sites.* Journal of the American Chemical Society, 2004. **126**(48): p. 15711-15719.

40. Velarde, M., R. Huber, S. Yanagisawa, C. Dennison, and A. Messerschmidt, *Influence of Loop Shortening on the Metal Binding Site of Cupredoxin Pseudoazurin.* Biochemistry, 2007. **46**(35): p. 9981-9991.

41. Machczynski, M.C., H.B. Gray, and J.H. Richards, *An outer-sphere hydrogen-bond network constrains copper coordination in blue proteins.* Journal of Inorganic Biochemistry, 2002. **88**(3-4): p. 375-380.

42. Hay, M., J.H. Richards, and Y. Lu, *Construction and characterization of an azurin analog for the purple copper site in cytochrome c oxidase.* Proceedings of the National Academy of Sciences of the United States of America, 1996. **93**(1): p. 461-464.

43. Hay, M.T., M.C. Ang, D.R. Gamelin, E.I. Solomon, W.E. Antholine, M. Ralle, N.J. Blackburn, P.D. Massey, X. Wang, A.H. Kwon, and Y. Lu, *Spectroscopic characterization of an engineered purple Cu_A center in azurin.* Inorg. Chem., 1998. **37**(2): p. 191-198.

44. Nossal, N.G., and Heppel, Leon L., *The release of enzymes by osmotic shock from escherichia coli in exponential phase.* The Journal of Biological Chemistry, 1966. **241**(13): p. 3055-3062.

45. Rathore, A.S., Bilbrey, Robert E., and Steinmeyer, David E., *Optimization of osmotic shock procedure for isolation of a protein product expressed in E. coli.* Biotechnology Progress, 2003. **19**: p. 1541-1546.

46. Neu, H.C.a.H., Leon A., *The release of enzymes from Escherichia coli by osmotic shock and during the formation of spheroplasts.* The Journal of Biological Chemistry, 1965. **240**(9): p. 3685-3692.

47. Chain, P., J. Lamerdin, F. Larimer, W. Regala, V. Lao, M. Land, L. Hauser, A. Hooper, M. Klotz, J. Norton, L. Sayavedra-Soto, D. Arciero, N. Hommes, M. Whittaker, and D. Arp, *Complete genome sequence of the ammonia-oxidizing bacterium and obligate chemolithoautotroph Nitrosomonas europaea.* Journal of Bacteriology, 2003. **185**(9): p. 2759-2773.

48. Fridovich, I., *Superoxide Dismutases.* Annual Review of Biochemistry, 1975. **44**: p. 147-159.

49. Edwards, R.A., Baker, Heather M., Whittaker, Mei M., Whittaker, James W., Jameson, Geoffrey B., Baker, Edward N., *Crystal structure of Escherichia coli manganese superoxide dismutase at 2.1 angstrom resolution.* Journal of Biological Inorganic Chemistry, 1998. **3**: p. 161-171.

50. Fridovich, I., *Quantitative aspects of the production of superoxide anion radical by milk xanthine oxidase.* The Journal of Biological Chemistry, 1970. **245**(16): p. 4053-4057.

51. Worthington, V., *Enzymes and related biochemicals.* Worthington Biochemical Corporation Manual, 1993.

52. McCord, J.M.a.F., Irwin, *Superoxide Dismutase: An enzymic function for erythrocuprein (hemocuprein).* The Journal of Biological Chemistry 1969. **244**(22): p. 6049-6055.

53. Suksrichavalit, T., S. Prachayasittikul, C. Nantasenamat, C. Isarankura-Na-Ayudhya, and V. Prachayasittikul, *Copper complexes of pyridine derivatives with superoxide scavenging and antimicrobial activities.* European Journal of Medicinal Chemistry, 2009. **44**(8): p. 3259-3265.

54. Devereux, M., M. McCann, D. O'Shea, M. O'Connor, E. Kiely, V. McKee, D. Naughton, A. Fisher, A. Kellett, M. Walsh, D. Egan, and C. Deegan, *Synthesis, superoxide dismutase mimetic and anticancer activities of metal complexes of 2,2-dimethylpentanedioic acid (2dmepdaH2) and 3,3-dimethylpentanedioic acid (3dmepdaH2): X-ray crystal structures of [Cu(3dmepda)(bipy)]2·6H2O and [Cu(2dmepda)(bipy)(EtOH)]2·4EtOH (bipy = 2,2'-bipyridine).* Bioinorg. Chem. Appl., 2006: p. 8/1-8/11.

55. Devereux, M., D. O'Shea, M. O'Connor, H. Grehan, G. Connor, M. McCann, G. Rosair, F. Lyng, A. Kellett, M. Walsh, D. Egan, and B. Thati, *Synthesis, catalase, superoxide dismutase and antitumor activities of copper(II) carboxylate complexes incorporating benzimidazole, 1,10-phenanthroline and bipyridine ligands: X-ray crystal structures of [Cu(BZA)2(bipy)(H2O)], [Cu(SalH)2(BZDH)2] and [Cu(CH3COO)2(5,6-DMBZDH)2] (SalH2 = salicylic acid; BZAH = benzoic acid; BZDH = benzimidazole and 5,6-DMBZDH = 5,6-dimethylbenzimidazole).* Polyhedron, 2007. **26**(15): p. 4073-4084.

56. Van Buuren, K.J.H., B.F. Van Gelder, J. Wilting, and R. Braams, *Biochemical and biophysical studies on cytochrome c oxidase. XIV. Reaction with cytochrome c as studied by pulse radiolysis.* Biochim. Biophys. Acta, Bioenerg., 1974. **333**(3): p. 421-9.